JACS
JOURNAL OF THE AMERICAN CHEMICAL SOCIETY
Communication
pubs.acs.org/JACS

Selective Electrocatalytic Reduction of CO_2 to Formate by Water-Stable Iridium Dihydride Pincer Complexes

Peng Kang, Chen Cheng, Zuofeng Chen, Cynthia K. Schauer, Thomas J. Meyer,* and Maurice Brookhart*

Department of Chemistry, The University of North Carolina at Chapel Hill, Chapel Hill, North Carolina 27599, United States

Supporting Information

ABSTRACT: Iridium dihydride complexes supported by PCP-type pincer ligands rapidly insert CO_2 to yield κ^2-formate monohydride products in THF. In acetonitrile/water mixtures, these complexes become efficient and selective catalysts for electrocatalytic reduction of CO_2 to formate. Electrochemical and NMR spectroscopic studies have provided mechanistic details and structures of key intermediates.

In solar fuels formation—water splitting to give hydrogen or CO_2 reduction to CO, other oxygenates, or hydrocarbons—a key is electro- or photoelectrocatalyzed reduction of CO_2. Progress has been made in identifying electrocatalysts,[1] with the dominant product being CO in most systems.[2] A few molecular electrocatalysts yield formate/formic acid;[3] however, these catalysts are often accompanied by nonselective formation of CO and H_2 or operate with low efficiency. For example, the $[(\eta^5\text{-}Me_5C_5)Rh(bpy)Cl]^+$ (bpy = 2,2′-bipyridine) catalyst[3e] yields a 2:1 formate/H_2 mixture upon electrochemical reduction of CO_2 in 5% water/acetonitrile. In contrast, formate dehydrogenase[4] selectively reduces CO_2 to formate at the thermodynamic potential with a high turnover frequency of ca. 280 s^{-1}. Since formic acid could serve as a hydrogen storage material,[5] a precursor to methanol, or a fuel in its own right,[6] more efficient electocatalysts for selective conversion of CO_2 to formic acid are desirable.

The insertion of CO_2 into metal−hydrogen bonds[7,8] has recently received attention, particularly in connection with hydrogenation of CO_2.[7a−f] Nozaki and co-workers[7c] have shown that the six-coordinate, 18-electron Ir(III) pincer trihydride complex **1** (Scheme 1) reacts with CO_2 in tetrahydrofuran (THF) at 25 °C to yield the formate complex $\mathbf{1}^{CO2}$. Under 1 atm CO_2, **1** and $\mathbf{1}^{CO2}$ are in equilibrium and present in approximately equal concentrations. Hazari and co-workers[7d] reported that six-coordinate Ir(III) pincer trihydride **2** inserts CO_2 to yield $\mathbf{2}^{CO2}$, in which formation of the adduct is driven by formation of a hydrogen bond as shown. A density functional theory (DFT) study by these authors suggested that insertion of CO_2 into six-coordinate Ir(III) trihydrides is normally endothermic. Both the Nozaki and Hazari systems hydrogenate CO_2 to formate under basic conditions. We report here that five-coordinate, 16-electron Ir(III) pincer dihydrides readily insert CO_2 and can be used as electrocatalyts for the selective reduction of CO_2 to formate or formic acid.[8]

Treatment of either $(POCOP)IrH_2$ (**3**) or $(PCP)IrH_2$ (**4**) with CO_2 (1 atm) in THF at 25 °C rapidly yields the corresponding κ^2-formate complexes $\mathbf{3}^{CO2}$ and $\mathbf{4}^{CO2}$, as shown in Scheme 1. $\mathbf{3}^{CO2}$ exhibits a formyl proton resonance at 9.3 ppm correlated to a carbon resonance at 173 ppm in $^1H-^{13}C$ HMQC spectra (additional NMR data are summarized in the SI[9]). Purging these solutions with Ar at 25 °C results in CO_2 loss and regeneration of **3** and **4**. The second-order rate constants for formation of these adducts, k_1, were determined at −65 °C, and the data are summarized in Table 1. The first-order rate constants for loss of CO_2 from the formate chelates, k_{-1}, were determined by preparing the adducts using $^{13}CO_2$ in THF, cooling to −65 °C, purging with Ar to remove excess $^{13}CO_2$ from solution, and then adding a large excess of CO_2. The rates of labeled $^{13}CO_2$ loss from the adducts (k_{-1}) followed first-order kinetics, as expected. Determination of the rate constants k_{-1} over a series of temperatures between 0 and −20 °C and subsequent Eyring analysis provided the $\Delta H^{\ddagger}$ and $\Delta S^{\ddagger}$ values summarized in Table 1. Extrapolation of the first-order rate constants k_{-1} to the temperature where the second-order rate constants k_1 were determined provided equilibrium constants, K_{eq}, corresponding to ΔG values of −5.9 kcal

Scheme 1. CO_2 Insertion by Ir Pincer Hydrido Complexes

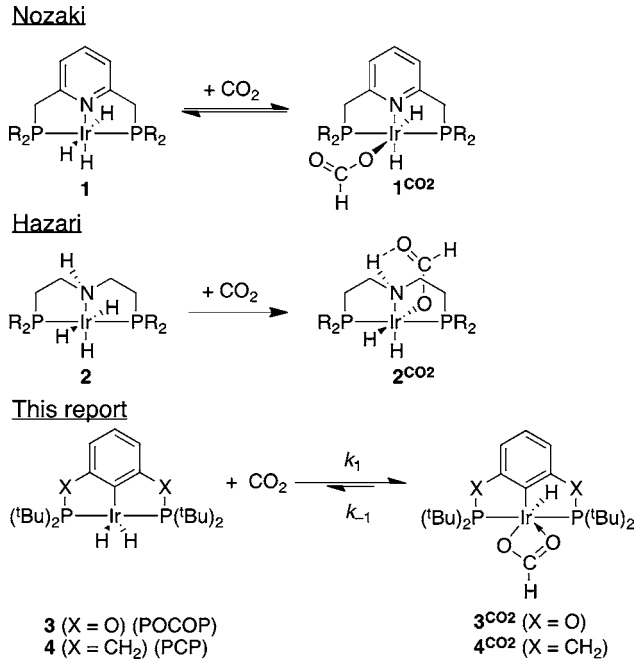

Received: January 17, 2012
Published: March 5, 2012

   dx.doi.org/10.1021/ja300543s | J. Am. Chem. Soc. 2012, 134, 5500−5503

Table 1. Kinetic and Thermodynamic Data for the Reactions of CO_2 with 3 and 4 in THF-d_8 at Low Temperatures[a]

	3	4
$k_{1,208K}$ (M^{-1} s^{-1})[b]	4.4(2) × 10^{-4}	1.00(8) × 10^{-2}
$\Delta G^{\ddagger}_{1,208K}$ (kcal mol^{-1})	15.3(2)	14.0(2)
$k_{-1,273K}$ (s^{-1})	5.7(6) × 10^{-4}	1.2(1) × 10^{-3}
$\Delta H^{\ddagger}_1$ (kcal mol^{-1})	25(2)	28(2)
$\Delta S^{\ddagger}_1$ (cal mol^{-1} K^{-1})	19(4)	30(10)
$K_{eq,208K}$ (M^{-1})	1.6(9) × 10^{6}	1.3(9) × 10^{8}
ΔG_{208K} (kcal mol^{-1})	−5.9(4)	−7.7(6)

[a]Errors shown represent two standard deviations. [b]The CO_2 concentration in 1 atm CO_2 saturated THF at 208 K is 5.6 M by quantitative ^{13}C NMR analysis.

mol^{-1} for **3** and −7.7 kcal mol^{-1} for **4** at −65 °C. These energetically favored insertions are apparently driven by stabilization through κ^2-chelation, an option unavailable to six-coordinate hydrides.[10]

Electrocatalytic reduction of CO_2 to formate was achieved by using **3** as the catalyst. In the cyclic voltammogram (CV) in MeCN with 5% H_2O (v/v, 0.1 M $^nBu_4NPF_6$) saturated by 1 atm CO_2 (Figure 1 left),[11] an electrocatalytic onset for CO_2

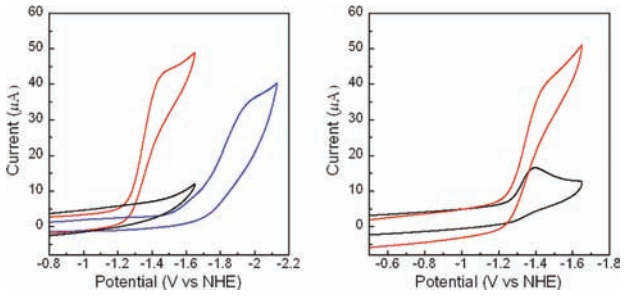

Figure 1. Left: CVs of 1 mM **3** in MeCN under Ar (black) or 1 atm CO_2 (red) and in THF under 1 atm CO_2 (blue). Right: CVs of 1 mM **3a**$^+$ under Ar (black) and CO_2 (red) in MeCN. Conditions: glassy carbon electrode, 7.1 mm^2, 5% H_2O, 0.1 M $^nBu_4NPF_6$, 100 mV s^{-1}, room temperature.

reduction appears at ca. −1.2 V vs NHE. The onset is shifted to ca. −1.6 V in 5% H_2O/THF. In view of the more positive potential in MeCN/H_2O, it was the solvent system of choice for further electrochemical studies. Controlled-potential electrolysis at −1.45 V in 5% H_2O/MeCN for 25 h (glassy carbon, 7.1 mm^2) yielded formic acid as the predominant product upon acidic workup, with a turnover number of ca. 40 by NMR analysis and a Faradaic efficiency of 85%.[9] H_2 was found as a side product (15%) by headspace GC analysis; it was formed via a nonspecific background reduction of water by the electrode.[12] Notably, no detectable amount of CO was found (<1%). The catalytic current gradually decreased over the extended period of the electrolysis as the solution eventually became basic (apparent pH > 9). Similar to **3**, **4** exhibits a catalytic current in 5% H_2O/THF under CO_2, yet the onset potential occurs more negatively, at ca. −1.8 V vs NHE.

The redox-active species in the catalytic cycle was investigated by cyclic voltammetry. As shown in Figure 1 left, in 5% H_2O/MeCN (0.1 M $^nBu_4NPF_6$) under Ar in the absence of CO_2, **3** exhibits no significant reduction wave to the solvent limit at −1.7 V. Rather, two oxidation waves were found at anodic peak potentials ($E_{p,a}$) of 0.25 and 0.72 V vs NHE (Figure S1[9]). The lack of a reduction wave for **3** points to it as the "reduced" form. A cationic complex with a single hydrido ligand, [(POCOP)IrH(MeCN)$_2$](BAr$^F_4$) (**3a**·BAr$^F_4$), was synthesized[9] as an "oxidized" counterpart of **3**. Indeed, **3a**$^+$ exhibited an irreversible reduction wave at a cathodic peak potential ($E_{p,c}$) of −1.4 V in MeCN under Ar (Figure 1 right), coincident with the onset potential for electrocatalytic CO_2 reduction by **3**.

The peak current ($i_{p,c}$) for the reduction of **3a**$^+$ varies linearly with the square root of the scan rate ($\upsilon^{1/2}$) from 10 to 500 mV s^{-1} under Ar (Figure S2[9]), consistent with diffusional reduction. Following a reductive scan, oxidation waves reappear at $E_{p,a}$ = 0.25 and 0.72 V, characteristic of **3**, thus confirming electrochemical generation of **3** from **3a**$^+$. The integrated area of each oxidation wave is ca. 50% of that for the reduction wave at −1.4 V. On the basis of an internal comparison of the integrated currents, the oxidation waves at 0.25 and 0.72 V probably correspond to one electron each, accounting for net oxidation of one of the hydrido ligands; reduction of **3a**$^+$ at −1.4 V is overall a two-electron process. The latter is consistent with Ir(III) → Ir(I) reduction, which is supported by the result of a DFT calculation showing that the LUMO of **3a**$^+$ is predominantly iridium-centered (Figure S9[9]). There is precedent for two-electron Ir(III)/Ir(I) electrochemical reduction.[3e]

The electrochemical observations are consistent with a mechanism in which the catalyst resides largely as **3a**$^+$ in the electrocatalytic steady state, with **3** as the reactive form. Reduction of **3a**$^+$ remains irreversible even at higher scan rates (up to 1 V s^{-1}) in formally dry MeCN, suggesting rapid protonation of the Ir(I) intermediate to regenerate the iridium dihydride species, which is reactive toward CO_2.

The kinetics of the reaction between **3** and CO_2 was investigated by cyclic voltammetry in MeCN with 5% H_2O. Relative to $i_{p,c}$ for **3a**$^+$ under Ar, the peak current for **3** (or **3a**$^+$) under CO_2 (i_{cat}) is enhanced ca. 3.8-fold at a scan rate of 100 mV s^{-1}. The catalytic peak current (i_{cat}) varies linearly with the Ir concentration (Figure S3[9]), consistent with a mechanism for CO_2 reduction that is first-order in catalyst. When normalized for the scan rate ($i_{cat}/\upsilon^{1/2}$), the catalytic peak current increases with decreasing scan rate from 500 to 5 mV s^{-1} (Figure S4[9]), consistent with a catalytic process in which **3a**$^+$ is regenerated and reduced at the electrode. Rate constants were evaluated by measurements of peak current ratios with (i_{cat}) and without ($i_{p,c}$) CO_2 at saturation. In eq 1,[13] n is the electrochemical stoichiometry (assumed to be 2 for both the diffusional and catalytic currents), υ is the scan rate in V s^{-1}, F is the Faraday constant, and k_{cat} is the observable catalytic rate constant, or turnover frequency. From the plot of $i_{cat}/i_{p,c}$ versus $\upsilon^{-1/2}$ (Figure S4 right[9]), k_{cat} = 20(2) s^{-1} in MeCN with 5% H_2O at 25 °C and 1 atm CO_2. The dependence of k_{cat} on [CO_2] was not investigated.

$$\frac{i_{cat}}{i_{p,c}} = \frac{(RT)^{1/2}}{0.446(nF\upsilon)^{1/2}}(k_{cat})^{1/2} \quad (1)$$

As shown by the data in Figure 2 left, in addition to acting as a proton source, water plays a key role in the CO_2 reduction. From the plot of $i_{cat}/i_{p,c}$ versus [H_2O] (Figure 2 right), the catalytic rate increases with added water, reaching saturation at ca. 4%. In the absence of CO_2, there is no significant current enhancement with added H_2O up to 5% under Ar (Figure S5[9]). An NMR study showed that **3** is stable with added H_2O for

dx.doi.org/10.1021/ja300543s | J. Am. Chem. Soc. 2012, 134, 5500−5503

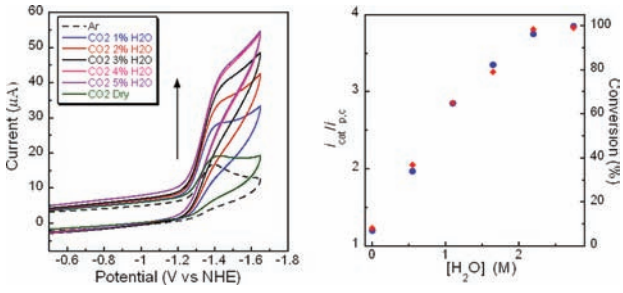

Figure 2. Left: CVs of 1 mM $\mathbf{3a}^+$ in MeCN with 0–5% added H_2O under CO_2 (glassy carbon electrode, 0.1 M $^nBu_4NPF_6$, 100 mV s^{-1}). Right: Plots of $i_{cat}/i_{p,c}$ (blue) and conversion of **3** to $\mathbf{3a}^+$ + formate by NMR (red) vs $[H_2O]$ in MeCN.

days. There is no evidence that **3** is catalytically active for water reduction to hydrogen.

An NMR investigation clarified the role of water in the overall CO_2 reduction mechanism. In anhydrous MeCN, **3** exists as a *six-coordinate* acetonitrile complex, (POCOP)Ir(H)$_2$(MeCN) ($\mathbf{3}^{MeCN}$), which forms no detectable insertion product under CO_2. When water is added, $\mathbf{3}^{MeCN}$ reacts with CO_2 to yield the cationic hydride $[(POCOP)IrH(MeCN)_2]^+$ ($\mathbf{3a}^+$), releasing formate anion, $HCOO^-$ (Scheme 2). There is a

Scheme 2. Reaction of (POCOP)IrH$_2$(MeCN) ($\mathbf{3}^{MeCN}$) with CO_2 in MeCN with Added H_2O

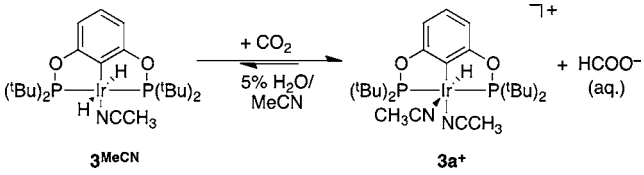

measurable equilibrium between $\mathbf{3}^{MeCN}$ and $\mathbf{3a}^+$ + $HCOO^-$, with the ionic reaction products present at >95% conversion with 4% added water (Figure 2 right and Figure S6[9]). The equilibrium in Scheme 2 is likely driven largely by stabilization of the formate anion by solvation and hydrogen bonding to water. Saturation at 4% water in the catalytic electrochemical reduction matches the "saturation" in the equilibrium formation of $\mathbf{3a}^+$, confirming $\mathbf{3a}^+$ to be the species that is reduced.

Scheme 3 shows an electrocatalytic mechanism consistent with the experimental observations. In acetonitrile, the dihydride exists as the acetonitrile adduct $\mathbf{3}^{MeCN}$. As shown above, $\mathbf{3}^{MeCN}$ is in rapid equilibrium with $\mathbf{3a}^+$, which likely forms via a κ^1-formate complex, $\mathbf{3}^I$.[14] At water concentrations above 4%, the dominant form of the catalyst in the electrocatalytic steady state is $\mathbf{3a}^+$. Two-electron, one-proton reduction of $\mathbf{3a}^+$ yields dihydride $\mathbf{3}^{MeCN}$. Water is the proton source, so hydroxide is generated and reacts with a second CO_2 to form bicarbonate, HCO_3^-.[15] Both $\mathbf{3}^{MeCN}$ and $\mathbf{3a}^+$ as the $BAr^F{}_4^-$ salts have been independently prepared and characterized.[9]

The results reported here provide quantitative data for insertion of CO_2 into five-coordinate iridium hydrides and a detailed mechanistic analysis of electrocatalytic CO_2 reduction by an Ir(III/I) hydride couple. There are two particularly notable features of these reductions in acetonitrile/water: (1) The catalysts are selective for reduction of CO_2 to formate. No CO is formed, and the small amount of hydrogen that is formed results from background reduction of water. The

Scheme 3. Proposed Mechanism for Electrocatalytic CO_2 Reduction with 3 in 5% H_2O/MeCN

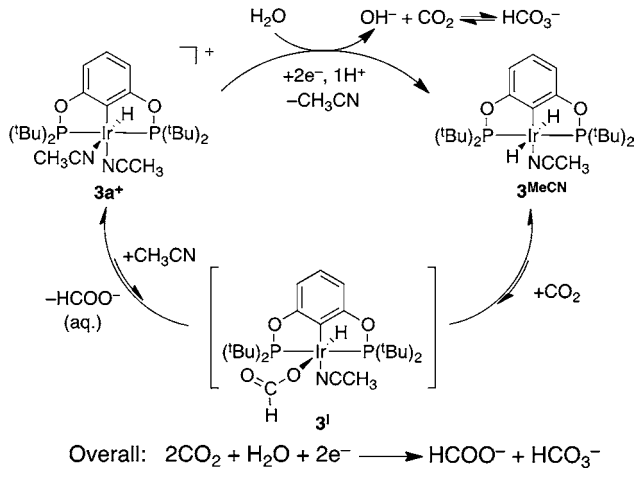

dihydrides are unreactive toward water under the conditions employed here for electrochemical experiments. (2) The role of the solvent is remarkable. Addition of water to $\mathbf{3}^{MeCN}$ in CH_3CN/CO_2 results in the formation of cationic $\mathbf{3a}^+$ and formate. Cationic $\mathbf{3a}^+$ is much more easily reduced than the neutral Ir(III) species. Thus, added water plays a critical role in lowering the reduction potential for electrocatalysis and minimizing background reduction of protons to H_2. These observations are potentially significant in the design of useful catalysts and procedures for generation of formate/formic acid in solar fuel schemes. We are expanding our investigations of this class of electrocatalysts for CO_2 reduction to further enhance the rates, lower the reduction potentials, and transfer the observed reactivity to electrode surfaces.

■ ASSOCIATED CONTENT

Supporting Information

Experimental and computational details, additional voltammograms and NMR data, bulk electrolysis, and product analysis. This material is available free of charge via the Internet at http://pubs.acs.org.

■ AUTHOR INFORMATION

Corresponding Author

tjmeyer@unc.edu; mbrookhart@unc.edu

Notes

The authors declare no competing financial interest.

■ ACKNOWLEDGMENTS

We thank Dr. Sabuj Kundu for the synthesis of **4** and gratefully acknowledge financial support of the UNC EFRC: Solar Fuels by DOE, Office of Science, Office of Basic Energy Sciences Award DE-SC0001011 (P.K., Z.-F.C.) and NSF as part of the Center for Enabling New Technologies through Catalysis (CENTC) CHE-0650456 (C.C.).

■ REFERENCES

(1) (a) Meyer, T. J. *Acc. Chem. Res.* **1989**, *22*, 163–170. (b) Leitner, W. *Angew. Chem., Int. Ed. Engl.* **1995**, *34*, 2207–2221. (c) Benson, E. E.; Kubiak, C. P.; Sathrum, A. J.; Smieja, J. M. *Chem. Soc. Rev.* **2009**, *38*, 89–99. (d) Mikkelsen, M.; Jorgensen, M.; Krebs, F. C. *Energy Environ. Sci.* **2010**, *3*, 43–81.

(2) (a) Beley, M.; Collin, J. P.; Ruppert, R.; Sauvage, J. P. *J. Chem. Soc., Chem. Commun* **1984**, 1315−1316. (b) Dubois, D. L.; Miedaner, A.; Haltiwanger, R. C. *J. Am. Chem. Soc.* **1991**, *113*, 8753−8764. (c) Hammouche, M.; Lexa, D.; Momenteau, M.; Saveant, J. M. *J. Am. Chem. Soc.* **1991**, *113*, 8455−8466. (d) Bruce, M. R. M.; Megehee, E.; Sullivan, B. P.; Thorp, H. H.; Otoole, T. R.; Downard, A.; Pugh, J. R.; Meyer, T. J. *Inorg. Chem.* **1992**, *31*, 4864−4873. (e) Smieja, J. M.; Kubiak, C. P. *Inorg. Chem.* **2010**, *49*, 9283−9289. (f) Bourrez, M.; Molton, F.; Chardon-Noblat, S.; Deronzier, A. *Angew. Chem., Int. Ed.* **2011**, *50*, 9903−9906. (g) Chen, Z. F.; Chen, C. C.; Weinberg, D. R.; Kang, P.; Concepcion, J. J.; Harrison, D. P.; Brookhart, M. S.; Meyer, T. J. *Chem. Commun.* **2011**, *47*, 12607−12609.

(3) (a) Slater, S.; Wagenknecht, J. H. *J. Am. Chem. Soc.* **1984**, *106*, 5367−5368. (b) Ishida, H.; Tanaka, H.; Tanaka, K.; Tanaka, T. *J. Chem. Soc., Chem. Commun* **1987**, 131−132. (c) Bolinger, C. M.; Story, N.; Sullivan, B. P.; Meyer, T. J. *Inorg. Chem.* **1988**, *27*, 4582−4587. (d) Arana, C.; Yan, S.; Keshavarzk, M.; Potts, K. T.; Abruna, H. D. *Inorg. Chem.* **1992**, *31*, 3680−3682. (e) Caix, C.; Chardon-Noblat, S.; Deronzier, A. *J. Electroanal. Chem.* **1997**, *434*, 163−170. (f) Rail, M. D.; Berben, L. A. *J. Am. Chem. Soc.* **2011**, *133*, 18577−18579.

(4) Reda, T.; Plugge, C. M.; Abram, N. J.; Hirst, J. *Proc. Natl. Acad. Sci. U.S.A.* **2008**, *105*, 10654−10658.

(5) Johnson, T. C.; Morris, D. J.; Wills, M. *Chem. Soc. Rev.* **2010**, *39*, 81−88.

(6) Rice, C.; Ha, R. I.; Masel, R. I.; Waszczuk, P.; Wieckowski, A.; Barnard, T. *J. Power Sources* **2002**, *111*, 83−89.

(7) (a) Jessop, P. G.; Ikariya, T.; Noyori, R. *Nature* **1994**, *368*, 231−233. (b) Jessop, P. G.; Joo, F.; Tai, C. C. *Coord. Chem. Rev.* **2004**, *248*, 2425−2442. (c) Tanaka, R.; Yamashita, M.; Nozaki, K. *J. Am. Chem. Soc.* **2009**, *131*, 14168−14169. (d) Schmeier, T. J.; Dobereiner, G. E.; Crabtree, R. H.; Hazari, N. *J. Am. Chem. Soc.* **2011**, *133*, 9274−9277. (e) Tanaka, R.; Yamashita, M.; Chung, L. W.; Morokuma, K.; Nozaki, K. *Organometallics* **2011**, *30*, 6742−6750. (f) Langer, R.; Diskin-Posner, Y.; Leitus, G.; Shimon, L. J. W.; Ben-David, Y.; Milstein, D. *Angew. Chem., Int. Ed.* **2011**, *50*, 9948−9952. (g) Creutz, C.; Chou, M. H. *J. Am. Chem. Soc.* **2007**, *129*, 10108−10109. (h) Chakraborty, S.; Zhang, J.; Krause, J. A.; Guan, H. *J. Am. Chem. Soc.* **2010**, *132*, 8872−8873. (i) Federsel, C.; Boddien, A.; Jackstell, R.; Jennerjahn, R.; Dyson, P. J.; Scopelliti, R.; Laurenczy, G.; Beller, M. *Angew. Chem., Int. Ed.* **2010**, *49*, 9777−9780. (j) Rankin, M. A.; Cummins, C. C. *J. Am. Chem. Soc.* **2010**, *132*, 10021−10023.

(8) (PCP)Rh(η^2-H_2) complexes have been shown to react with CO_2 (see a−c) and form stable κ^2-chelate complexes (see b and c): (a) Kaska, W. C.; Nemeh, S.; Shirazi, A.; Potuznik, S. *Organometallics* **1988**, *7*, 13−15. (b) Vigalok, A.; Ben-David, Y.; Milstein, D. *Organometallics* **1996**, *15*, 1839−1844. (c) Huang, K. W.; Han, J. H.; Musgrave, C. B.; Fujita, E. *Organometallics* **2007**, *26*, 508−513.

(9) See the Supporting Information (SI).

(10) (a) An Ir PCP-pincer κ^2-bicarbonate chelate has been crystallographically characterized and provides evidence in addition to the NMR data for the formation of κ^2-chelates. See: Lee, D. W.; Jensen, C. M.; Morales-Morales, D. *Organometallics* **2003**, *22*, 4744−4749. (b) The core atoms binding to Ir in a single crystal of $\mathbf{3}^{CO2}$ have been refined and support a κ^2 coordination mode, but disorder of the *tert*-butyl methyl groups prevented full refinement.

(11) The saturated CO_2 concentration in MeCN was determined to be 0.38 M by a quantitative single-pulse ^{13}C NMR experiment under 1 atm CO_2 at 25 °C. A CO_2 solubility of 0.28 M in MeCN obtained using a back-titration method was previously reported. See: Fujita, E.; Szalda, D. J.; Creutz, C.; Sutin, N. *J. Am. Chem. Soc.* **1988**, *110*, 4870−4871.

(12) Control experiments without **3** under identical conditions for 25 h produced more H_2 than with **3** added (see the SI for details).

(13) Zanello, P. *Inorganic Electrochemistry: Theory, Practice and Applications*; Royal Society of Chemistry: Cambridge, U.K., 2003.

(14) Exposing dihydride **4** in anhydrous MeCN to CO_2 yields the six-coordinate κ^1-complex (PCP)IrH(MeCN)$_2$(OOCH) ($\mathbf{4}^{I}$). Addition of water to this solution results in formate ionization to yield [(PCP)IrH(MeCN)$_2$]$^+$ ($\mathbf{4a}^+$) plus $HCOO^-$ (see the SI for characterizations). The observation of $\mathbf{4}^{I}$ suggests $\mathbf{3}^{I}$ as a possible intermediate in the conversion of $\mathbf{3}^{MeCN}$ to $\mathbf{3a}^+$.

(15) A bicarbonate resonance was observed at 162 ppm by ^{13}C NMR spectroscopy in the electrolysis solution without acidic workup. Upon the acidic workup, CO_2 was released, and the bicarbonate signal could no longer be observed.